

PI CONTROL APPLICATION FOR BUILDING AIR CONDITIONING SYSTEM

Henry Nasution,^{a,b,*} Azhar Abdul Aziz^a, Zulkarnain Abdul Latiff,^a

^aAutomotive Development Centre, Faculty of Mechanical Engineering, Universiti Teknologi Malaysia, 81310 UTM Johor Bahru, Johor, Malaysia

^bDepartment of Mechanical Engineering, Faculty of Industrial Technology, Universitas Bung Hatta, Padang 25132, Sumatera Barat, Indonesia

Article history

Received

14 Feb 2015

Received in revised form

11 March 2015

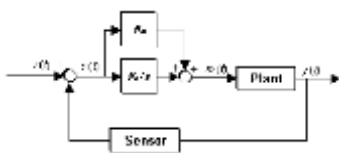
Accepted

25 March 2015

*Corresponding author

henry@fkm.utm.my

Graphical abstract



Abstract

This manuscript presents a PI controller implementation to control the compressor speed of an air conditioning system based on cooling load to fulfill thermal comfort requirements with higher energy efficiency. Hence, an interface was designed to monitor the experiment, including the controller algorithm. The temperature settings of the conditioned space were 20, 22, and 24°C with internal heat loads of 0 and 1000 W. The experiments conducted indicated that the proposed technique had better temperature control and energy efficiency compared to the thermostat controller.

Keywords: Performance; energy saving; air conditioning; pi control

Abstrak

Manuskrip ini membentangkan pelaksanaan pengawal PI untuk mengawal kelajuan pemampat sistem penyaman udara mengikut penyejukan beban untuk memenuhi keperluan keselesaan haba dengan kecekapan tenaga yang lebih tinggi. Oleh itu, antara muka telah direka untuk memantau eksperimen, termasuk algoritma pengawal. Tetapan suhu ruang yang dingin adalah 20, 22, dan 24°C dengan banyak haba dalaman 0 dan 1000 W. Eksperimen yang dijalankan menunjukkan bahawa teknik yang dicadangkan mempunyai kawalan suhu yang lebih baik dan kecekapan tenaga berbanding dengan pengawal termostat.

Kata kunci: Prestasi; penjimatan tenaga; penyaman udara; kawalan pi

© 2015 Penerbit UTM Press. All rights reserved

1.0 INTRODUCTION

The air conditioning (AC) systems play several roles to reduce the environmental impact on buildings. The primary function of AC systems is to provide healthy and comfortable interior conditions for occupants. The goal of AC control system design is to provide good control strategies to maintain comfort for the occupants of a building under variable load conditions with minimal use of energy. Therefore, reducing energy consumption becomes one of the most important aspects in AC control system design

because of the fact that 50% of the world energy is consumed by AC equipment in industrial and commercial buildings [1-4].

Control by varying the rotational speed of the compressor improves the general performance and regulates the rotational speed to the required refrigeration capacity [5-6]. In capacity control cooling application, the compressor speed influences various operating and design parameters, such as cooling capacity, power consumption, COP, volumetric, and isentropic efficiencies [7].

The variable speed in AC maintains the required temperature of the air conditioned space by means of an inverter, which varies the speed of the compressor with a controller. Actually, it is the cooling capacity matches the cooling load that varies at low load compressor runs at low speed, and hence, saves energy [8]. The basic difference between variable speed refrigeration and conventional refrigeration systems is in the control of the system capacity. In variable speed refrigeration, the capacity of the refrigeration system is matched to the load by regulating the speed of the compressor motor in such a way that the capacity of the system tracks the load dictated on it by varying operating conditions.

Besides, the variable load can be controlled by reducing the speed of the electric machine, which means applying less power to the system. As stated above, for the constant speed motor, the machine is set to the maximum level, and the machine works at that level regardless of the load. If the load increases, a higher motor speed is needed. However, adjustable speed drives can adjust the speed of the motor when the load changes, thereby reducing the applied power to the system [7].

With respect to these opportunities, the current research focused on energy and performance of an AC system using proportional-integral (PI). The main idea of designing the controller was to maximize energy-saving for an AC system application through variable speed drive control.

2.0 PI CONTROLLER

The majority of control systems in the world are operated using PID controllers. Indeed, it has been reported that 98% of the control loops in the pulp and paper industries are controlled by single-input single-output PI controllers and that in process control applications, more than 95% of the controllers are of PID type. Similar statistics hold in the motion control and aerospace industries [9], where PID is used for a wide range of problems: process control, motor drives, magnetic and optic memories, automotive, flight control, instrumentation, etc. [10].

Proportional control action is usually combined with integral control action to form the proportional-integral (PI) control action, described by:

$$m(t) = [K_p e(t)] + [K_i \int e(t) dt] \quad (1)$$

where $m(t)$ is control variable, K_p represents the proportional gain, error signal $e(t)$ and K_i represent the integral gain.

The PI control algorithm offers some of the advantages of both the proportional and integral algorithms. It is more difficult to tune the PI controller, because there are two gains to be adjusted. A proportional controller will have the effect on

reducing the rise time and will reduce, but never eliminates the steady state error. Meanwhile, an integral control will have the effect of eliminating the steady state error, but it may make the transient response worse. The use of proportional control requires just one variable to be selected, the proportional gain K_p , for the control system to have the required dynamic behavior. The use of a proportional gain plus integral gain (PI) controller requires the selection of two variables, K_p and K_i . Figure 1 shows the block diagram of a PI controller.

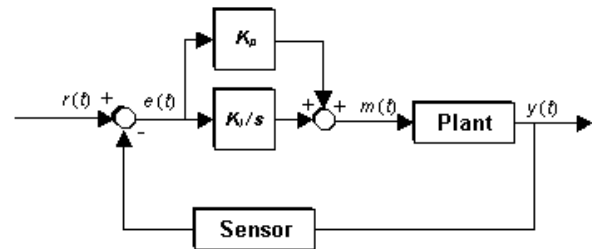


Figure 1 Block diagram of a PI control system

Referring to equation (1), the digital controller gains; K_p , K_i , and K_d , can be determined from the analogue controller gains by using the following relationships [11-13]:

$$K_p = K_p \quad (2)$$

$$K_i = K_i' \Delta t \quad (3)$$

The PI algorithm can be written as:

$$P = [K_p' \text{Error}] \quad (4)$$

$$PI = [K_p' \text{Error}] + [K_i'] \quad (5)$$

where

$$\text{Error} = \text{setpoint} - \text{measurement point} \quad (6)$$

$$\Delta \text{Error} = [\text{Error}_n - \text{Error}_{n-1}] \quad (7)$$

Δt : sampling interval

The PI parameters, K_p and K_i , need to be adjusted for optimum system performance and this process is called tuning. Controller tuning means the process of adjusting the controller parameter of the proportional action, integral action, and derivative action to achieve the desired system performance. The basic principle of tuning is to set the time and the controller parameters of the controller to fit the time and parameters (called dynamics) of the process. When tuning, generally, it is necessary to upset the process [14]. For controller tuning, simplicity, as well as optimality, is important. The three modes of the ordinary PI controller, K_p and K_i , do not readily translate into the desired performance and robustness characteristics, which the control system designer has

in mind. The presence of simple rule that relates model parameters and/or experimental data to controller parameters serve to simplify the task of the designer [15].

3.0 COEFFICIENT OF PERFORMANCE (COP) OF REFRIGERATION CYCLE

The COP of refrigeration machine is the ratio of the energy extracted by the evaporator (refrigerating effect) to energy supplied to the compressor. Thus, using the notations in Figure 2, the formula given is:

$$COP = \frac{(h_1 - h_4)}{(h_2 - h_1)} = \frac{Q_e}{W_{com}} \tag{8}$$

COP is a dimensionless index used to indicate the performance of a thermodynamic cycle or thermal system. The magnitude of COP can be greater than 1.

For the Carnot refrigeration cycle:

$$COP_{carnot} = \frac{Q_e}{Q_c - Q_e}$$

$$COP_{carnot} = \frac{T_1(s_1 - s_4)}{(T_2 - T_1)(s_1 - s_4)} = \frac{T_1}{T_2 - T_1} \tag{9}$$

where Q_e is refrigeration effect (kJ/kg), work input to the compressor W_{com} (kJ/kg), h_1 and h_4 (kJ/kg) are the enthalpy of refrigerant at state points 1 and 4, h_2 (kJ/kg) is the enthalpy of refrigerant at state point 2, Q_c is heat rejection during condensation (kJ/kg.K), s_1 and s_4 (kJ/kg.K) are the entropy of refrigerant at state points 1 and 4, T_1 (°C) is temperature at state point 1, and T_2 (°C) is temperature at state point 2.

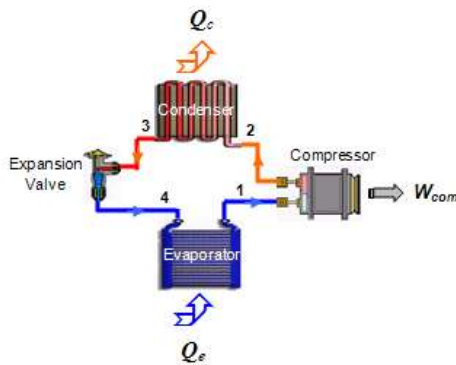


Figure 2a Schematic diagram

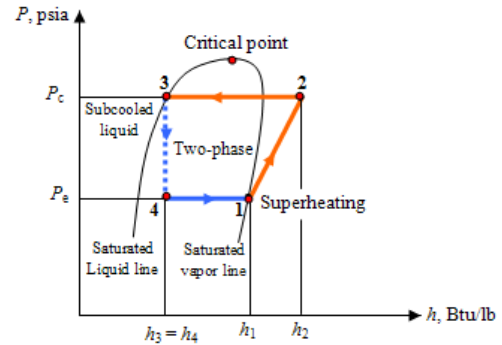


Figure 2b P - h diagram

4.0 POWER AND ENERGY

The general equation for the output power (P) from a three-phase induction motor is given as:

$$P = \frac{I \times V \times PF \times 1.73}{1000} \text{ (kW)} \tag{10}$$

where I is current (Amperes), V is voltage (Volts), and PF is power factor.

Using equation (10), approximately the PF can be calculated from the motor name plate data as follows [16]:

$$PF = \frac{431 \times hp}{E \times I \times Eff} \tag{11}$$

where hp is the rated horsepower (hp), E is the rated voltage (Volts), and Eff is the per unit motor efficiency (0.80) [16].

In obtaining the energy consumed, the motor power from equation (10) is multiplied by the time of operation, t (minute) and is given as:

$$\text{Energy} = P \times t \tag{12}$$

5.0 EXPERIMENT SETUP AND PROCEDURE

5.1 Thermal Environmental Room and Air Handling Unit (AHU)

This research involved the implementation of a standard thermal environmental room using an AC unit. The room had been located in the Thermodynamic Laboratory of Mechanical Engineering Faculty, Universiti Teknologi Malaysia, with low ventilation and unexposed to solar radiation.

A standard thermal environmental room of size 4.5 m long, 3.28 m wide, 3.43 m high, and 50.63 m3 volume had been used. The construction of the room is illustrated in Figure 3. The four-sided walls were constructed with 105 mm thickness of concrete

blocks, 125 mm thickness of fiberglass insulation panels, and laminated with 10 mm thickness of perforated hardboard. The floor and ceilings were cemented with sand and gravel of 180 mm thickness. The room was constructed with only one door and was facilitated with 4 fluorescent lights of power 36 W each, a pair of air diffusers, and 2 return air duct system.

A small type of AC system was located outside the thermal environmental room. The system comprised of TD.31a bench (refrigeration unit) and TD.31 bench (air handling unit) that made a complete system. At AHU, the return air from the thermal room was sucked through the return duct system and mixed with some outside air. As the air passed through the evaporator, the heat from return air was transferred to the tubes. This Direct Expansion (DX) type evaporator had the capacity of 8.31 kW and was capable of supplying up to 43 m³/min of maximum air volume. The return air then flowed through the supply duct system and was blown back to the room by a 375 W (0.5 hp) supply axial fan, with a two-speed (low and high speed) set point.

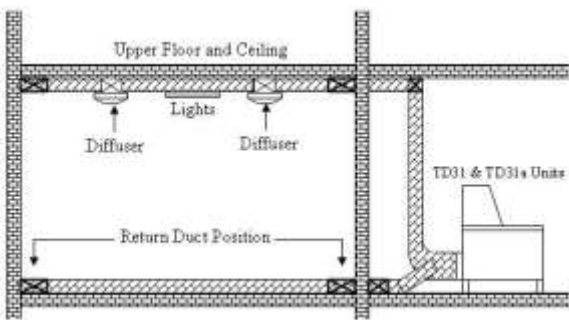


Figure 3a Side View

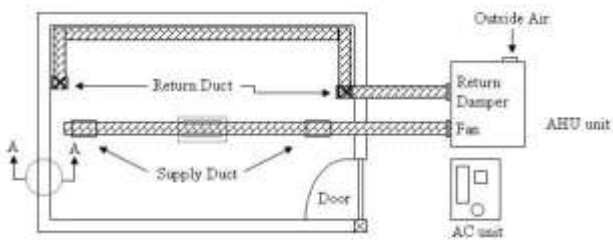


Figure 3b Plan View

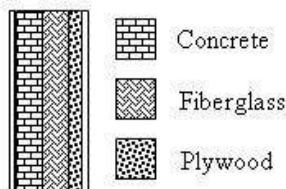


Figure 3c Plan View

Figure 3 The construction of thermal environmental room

The compression process began as the R12 vapor entered the reciprocating compressor. The compressor was belt driven by 3 kW (4 hp) electric motor at 1420 rpm, and electrical supply of 440 V, 3 phase, 50 Hz, 6.5 A. After the compression process, the R12 was discharged at high temperature and pressure. The condensation process took place as it passed through the water-cooled condenser. Here, R12 vapor was converted back to liquid. Using water as the condensing medium, a cooling tower, located at about 7 meters away from the refrigerating unit bench was used for final heat rejection to the atmosphere.

5.2 Experimental Equipment

A schematic diagram of the experimental rig is shown in Figure 4. This figure shows the arrangement of the instruments and the configuration of the flow of the system. The installation of the hardware began by placing six T-type thermocouple sensors (points: T1, T2, T3, T4, T5, and T6), and four pressure gages (points: P1, P2, P3, and P4) in the AHU and refrigerating unit to the respective places. Besides, five of ICs temperature sensors were placed on the opposite walls in the thermal environmental room (points: T7, T8, T9, T10, and T11), in which the average value of the room temperature was taken.

The control system of the compressor speed consisted of an ICs temperature sensors in thermal environmental room, a PI subroutine was installed to the computer, while an inverter and an electrical motor were coupled to the compressor. The ICs temperature sensor monitored the temperature of the room and emitted electrical signals proportional to the state of the conditioned space. This signal was filtered before it reached the controller, thus minimizing noise, which might cause error in the control system. The output signal was supplied to the controller and computer, which sent out a control signal that was a function of the error between the value of the monitored temperature and the required set point temperature. The control signal output was supplied to the inverter, which modulated the electrical frequency supplied to the motor such that it was linearly proportional to the control signal. Electricity of 50 Hz was supplied to the inverter, which supplied variable-frequency electricity to the motor. Besides, the rotational speed of the motor was directly proportional to the frequency of the electricity supplied to the motor.

A common signal conditioning and analog input channel was used to read all sensors/transducers, such as one analog input from inverter, five ICs temperature sensors from thermal environmental room, and six thermocouples from AC unit. The sensors/transducers provided voltages to the analog channels of a multiplexer. The multiplexer selected one of these channels at a time and sent that signal on to TC-08 and PCI-1711, which fed binary number to the PC for data processing. The variable speed software was facilitated by displaying and recording

the data. The input setting directly used the operational amplifier switch of the inverter.

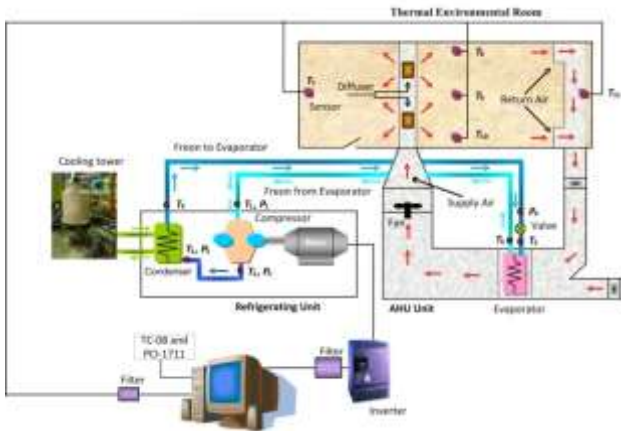


Figure 4 The experimental setup

5.3 Experimental Planning

The objective of conducting tests on the variable speed control of the compressor system was to analyze the actual working performance, energy consumed, and the potential energy saving. The performance tests for variable speed control system were conducted based on different temperature settings and internal heat loads. The room temperature was controlled by using on/off and PI controller.

The experiments were conducted at two different conditions:

1. The compressor system test with on/off controller
2. The variable speed of compressor system test with PI controller.

The experimental settings were:

1. Temperature setpoints = 20, 22, and 24°C.
2. Internal heat loads = 0 and 1000 W.

With the implementation of variable speed drive connected to the compressor motor, thermocouple wire sensor, data acquisition modules, and a personal computer were the items included in the hardware design. The data acquisition and the control process were the programs developed under the software section. Thus, with the integration of hardware and software systems, the design requirements to facilitate the systems with the following function had been expected to be successfully determined. The requirements were:

1. Setting the room temperature setpoint for variable speed control.
2. Sensing temperature of the room.

3. Displaying and recording data of room temperature, AHU, and electrical motor.
4. Controlling motor frequency or speed depending on cooling load.
5. Measuring the energy consumption of the motor compressor.

6.0 RESULTS AND DISCUSSION

6.1 Variable Speed Performance

6.1.1 Temperature Distribution

The performance test on variable speed motor had been conducted at various frequencies from 20 to 50 Hz. The temperatures of the room and AHU, pressure of AC system, and power of the electrical motor were recorded. The experiment was conducted to study the effect of frequency variation.

Figure 5 shows the room temperature variations for various motor frequencies. The room temperature was frequency dependent. The data gathered showed that the higher the frequency, the lower is the room temperature. Meanwhile, Table 1 shows the steady state values of the room temperature for all frequencies tested. The rate of decrease in the temperature until the steady state condition had been different for each speed, indicating that the cooling rate and the time to reach a steady state had varying temperatures. For this system, the steady state temperature varied from 18.45 to 25.64°C.

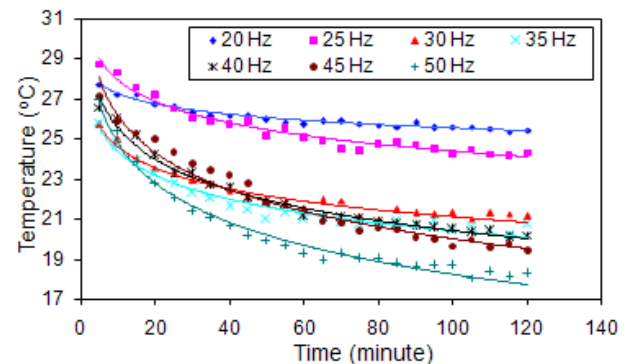


Figure 5 Room temperature at various frequencies

Table 1 Steady state values of room temperature at various frequencies

Frequency (Hz)	20	25	30	35	40	45	50
Room temperature (°C)	25.64	24.49	21.39	20.65	20.53	19.66	18.45

6.1.2 Energy Consumption

Figure 6 shows the effect of motor frequencies on the steady state value of the room temperature and the

energy consumption during the test period. Energy consumption was calculated from the start of the motor using the relationship given by equation (12). The data indicated that the room temperature of the AC system was dependent on the motor frequency. When the frequency increased, the room temperature decreased, while the energy consumption increased.

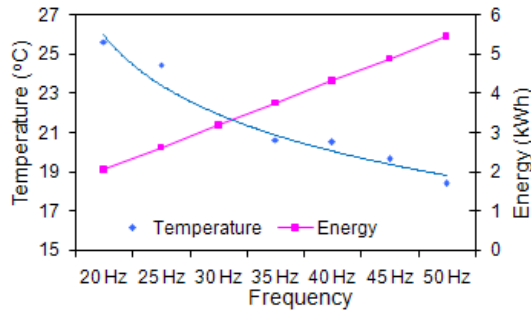


Figure 6 Steady state room temperature and energy consumption at various frequencies

6.1.3 Coefficient of Performance

Figure 7 shows the variation of actual and Carnot COP. A high COP at a lower frequency was mostly due to the small compressor power consumption compared with that at a higher frequency. When the compressor power consumption increased, the COP decreased with the increase of the compressor frequency. When the compressor that operated the frequency increased, the evaporating temperature decreased, and the superheat of the refrigerant before the compressor inlet increased.

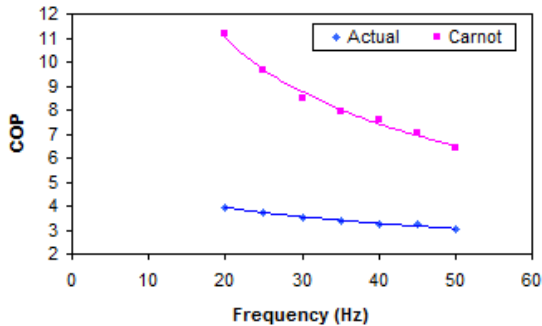


Figure 7 Steady state of Actual and Carnot COP at various frequencies

6.2 On/off Control

6.2.1 Temperature Distribution

Figures 8-10 show the motor speed and the temperature response at various temperature settings. The controller turned on the motor compressor when the room temperature reached the upper limit temperature setting, and turned off at the lower limit temperature setting. If the temperature setting was

low and the internal heat loads were high, then the time needed to reach the required room temperature was longer. As a consequence, a longer time was needed for the controller to turn off the motor compressor. After the controller turned off the motor compressor, when the internal heat loads increased, then the time for the controller to turn on the motor compressor was faster. This action was taken to allow a faster heat recovery to the room until the temperature setpoint was upheld again.

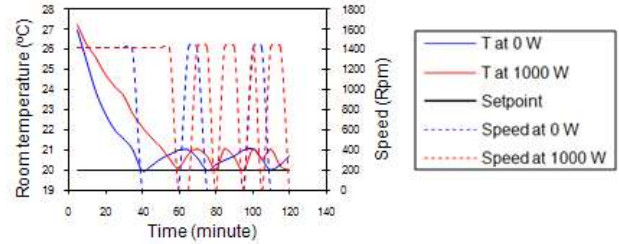


Figure 8 Motor speed and temperature responses Tsetpoint = 20°C

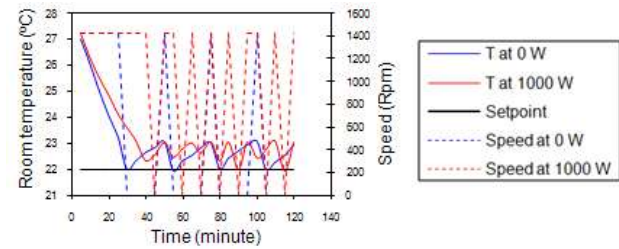


Figure 9 Motor speed and temperature responses Tsetpoint = 22°C

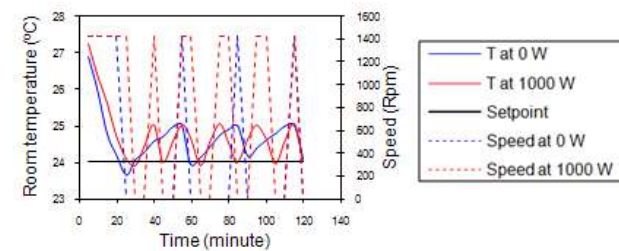


Figure 10 Motor speed and temperature responses Tsetpoint = 24°C

6.2.2 Energy Consumption

Figure 11 shows the energy consumption at various temperature settings and internal heat loads. The time needed for each temperature setting is given in Table 4.4. The time to reach the required temperature had influence on the electrical energy consumption. Energy consumption was calculated from the start of the motor using the relationship given by equation (12). The following had been observed from Figure 11:

1. The longer the motor compressor ran, the higher was the energy consumption.

2. The smaller the setpoint temperature, the higher was the energy consumption.
3. The higher the internal heat load, the higher was the energy consumption.

6.2.3 Coefficient of Performance

Table 2 shows the average value for actual and Carnot COP for all temperature settings. The average actual COP was 3.06. On the other hand, the average Carnot COP was 6.92. The results denoted that the value of COP for Carnot was higher than the actual COP. This indicated that the process had been designed correctly.

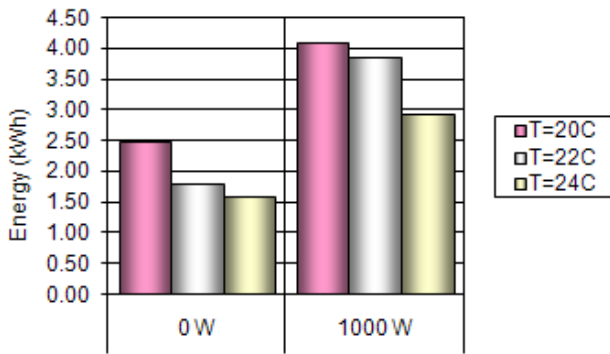


Figure 11 The energy consumption distribution for on/off control

Table 2 The average value of actual and Carnot COP

Temperature Setting	Actual		Carnot	
	0 W	1000 W	0 W	1000 W
T=20°C	3.06	3.06	6.92	6.92
T=22°C	3.06	3.06	6.92	6.91
T=24°C	3.06	3.06	6.92	6.91

6.3 PI Control

6.3.1 Temperature Distribution

Figures 12-14 show the motor speed and the temperature responses at various temperature settings and PI controller. Initially, the motor was set to run at the maximum speed (50 Hz). With the maximum compressor motor speed, the room temperature decreased as the time increased. Referring to the setpoint temperature, the controller minimized the error between the setpoint and the room temperatures. The figures also show that the motor speeds dropped abruptly as the room temperatures reached the setpoint. This action was taken to allow a faster heat recovery to the room until the temperature setpoint was upheld again. The controller manipulated the motor speed so that the room

temperature was at or close to its setpoint temperature.

6.3.2 Energy Consumption

Figure 15 shows the energy consumption at various temperature settings and internal heat loads for all the controller modes. Energy consumption was calculated from the start of the motor using the relationship given by equation (12). The results indicated that:

1. The smaller the setpoint temperature, the higher was the energy consumption.
2. The higher the internal heat loads, the higher was the energy consumption.

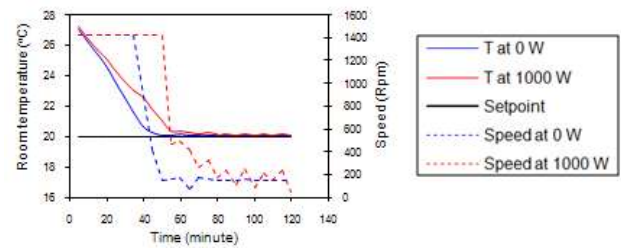


Figure 12 Motor speed and temperature responses at Tsetpoint = 20°C for PI control

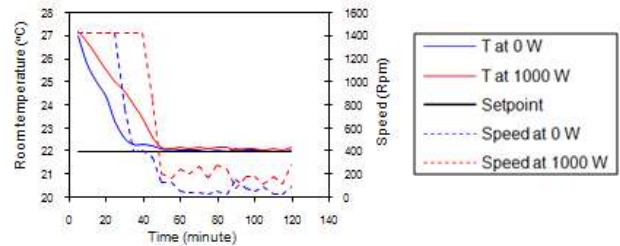


Figure 13 Motor speed and temperature responses at Tsetpoint = 22°C for PI control

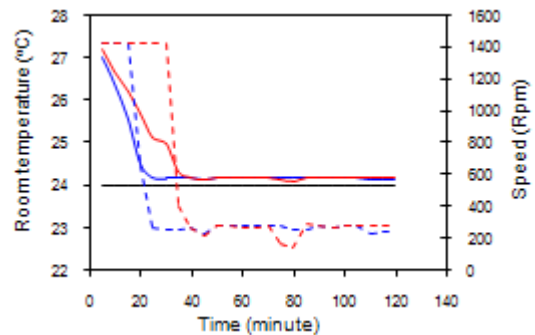


Figure 14 Motor speed and temperature responses at Tsetpoint = 24°C for PI control

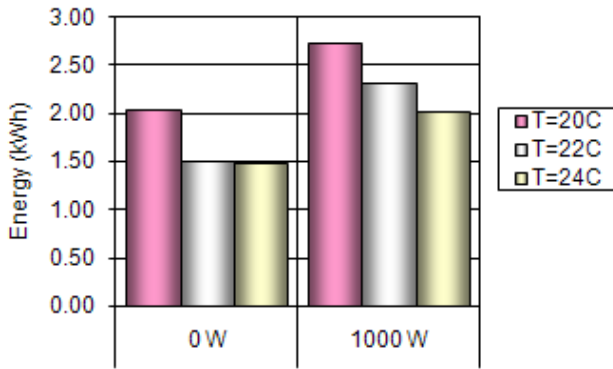


Figure 15 The energy consumption distribution for PI control

6.3.3 Coefficient of Performance

Figure 16 illustrates the relationship between the coefficient of performance between actual and Carnot with frequency. The higher the frequency, the smaller was the value of COP (actual and Carnot). The average values of the actual and the Carnot COP were found to be 3.05 to 4.34, and 6.88 to 11.39, respectively for PI controller. A high COP at the low frequency was mostly due to the small compressor power consumption compared with that at higher frequencies. When the compressor power consumption increased, the COP decreased with the increase of the compressor frequency.

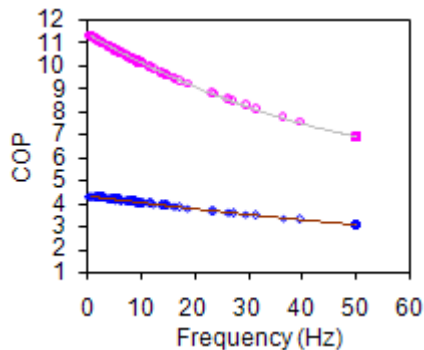


Figure 16 The actual and Carnot COP for PI control

6.4 Energy Saving Analysis

Meanwhile, energy consumption was calculated by multiplying the power consumption of the motor by the actual operating hours given by equation (12). The power and energy consumption were calculated every five minutes. The results summarized the energy consumption for two-hour operation periods for each temperature setting and internal heat load.

The energy saving calculated is expressed in terms of savings in percentage unit, based on the difference between energy consumed by on/off controller and energy consumed by PI controller. The equation is given as :

$$\text{Energy saving} = \frac{(\text{On/Off energy}) - (\text{PI energy})}{(\text{On/Off energy})} \times 100 \quad (13)$$

Figure 17 shows the energy consumed and energy saved for PI controller in comparison with on/off controller. The figure shows that the energy consumption had been varied with different internal heat loads and different temperature settings. If the temperature setting was low and the internal heat loads were high, then the energy consumption was high. Furthermore, the higher the energy consumption, the smaller was the energy saving. Moreover, for continuous two-hour use, the energy savings achieved by running the system at various internal heat loads (0 and 1000 W) and various temperatures setting (20, 22 and 24°C) were 18.46 to 33.29%, 16.99 to 40.11%, and 5.97 to 31.68% for PI control.

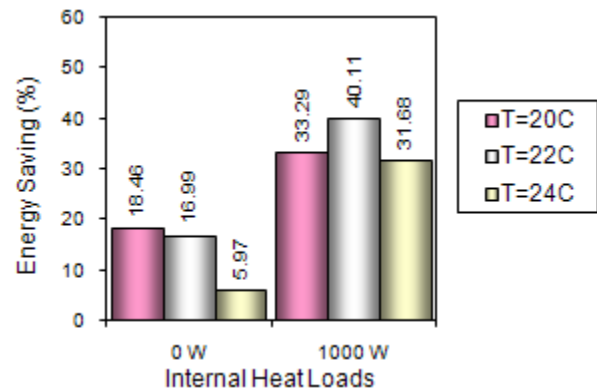


Figure 17 Energy saving distribution: on/off – PI controller

7.0 CONCLUSION

The existing AC system that was operated using constant speed system produced a very low room temperature, which was below comfort temperature as time increased. The controllers, i.e. on/off and PI developed, were to control the motor speed in order to maintain the room temperature at or close to the setpoint temperature. The on/off controller was used in many simple control systems, the controller turn on (1420 rpm) the motor compressor when the room temperature reached the upper limit temperature setting, and turn off (0 rpm) at lower limit temperature setting. Besides, the PI controller tried to minimize the error between the setpoint temperature and the room temperature. If the room temperature reached the setpoint, the motor speed was abruptly reduced and fluctuated to maintain the room temperature. However, when the room was thermal loaded, the controllers acted such that the heat recovery to the room was faster until the temperature setpoint was upheld again. The speed variation for the controlled system was found to be between 0 and 500 rpm. The

energy consumption would change with the change in the motor speed. When the motor speed increased, the room temperature decreased and COP increased with the increase in energy consumption. Furthermore, the higher the energy consumption, the smaller was energy saving.

Hence, the application of variable speed system to AC offers a potential for substantial energy savings or energy efficiency. The investigation indicated that the room temperature might be controlled by inverter driven motor to achieve energy saving.

References

- [1] M.S.Imbabi. 1990. Computer validation of scale model tests for building energy simulation. *International Journal of Energy Research*. 14723-736.
- [2] J.Hensen. 1995. On system simulation for building performance evaluation. Proceeding of the 4th IBPSA World Congress "Building Simulation'95". Wisconsin. 259-267.
- [3] H. Nasution, M. N. W. Hassan. 2006. Potential electricity savings by variable speed control of compressor for air conditioning systems. *Clean Technology Environment Policy*. 8: 105-111.
- [4] H. Nasution, K. Sumeru, A. A. Aziz, M. Y. Senawi. 2014. Experimental study of air conditioning control system for building energy saving. *Energy Procedia*. 61: 63-66.
- [5] R. N .N.Koury, L.Machado, K. A. R.Ismail. 2001. Numerical simulation of a variable speed refrigeration system. *International Journal of Refrigeration*. 24192-200.
- [6] M.Takebayashi, K.Sekigami, I.Tsubono, H.Kohsokabe, K.Suefuji, K.Inaba. 1994. Performance improvement of a variable speed controlled scroll compressor for household air conditioners. *ASHRAE Transactions*. 100(1): 471-475.
- [7] S. A.Tassou, T.Q. Qureshi. 1998. Comparative performance evaluation of positive displacement compressors in variable speed refrigeration applications. *International Journal of Refrigeration*. 21(1): 29-41.
- [8] M. Afandi. 2004. Energy Saving in an Air-Conditioning System Using an Inverter and a Temperature-Speed Controller, Universiti Teknologi Malaysia, Malaysia.
- [9] P. S. R.Diniz, A. B. D. Silva, S. L.Netto. 2002. Digital Signal Processing System Analysis and Design, Cambridge, United Kingdom
- [10] K. J. Astrom. 1988. T.Hagglund, Automatic Tuning of PID Controllers. Instrument Society of America United States of America
- [11] K. I.Krakow, S.Lin, Z. S. Zeng. 1995. Temperature and humidity control during cooling and dehumidifying by compressor and evaporator fan speed variation. *ASHRAE Transactions*. 101(1): 292-304.
- [12] C. G. Nesler. 1986. Automated controller tuning for HVAC applications. *ASHRAE Transactions*. 92(2B): 1541-1552.
- [13] G. A.Perdikaris. 1991. *Computer Controlled Systems Theory and Applications*, Kluwer Academic Publisher, Netherlands,
- [14] D. W. S.Clair, P. S.Freuhauf. 1994. PID Tuning: It's the method, not the rules. *Intech Engineer's Notebook*. 26-30.
- [15] D. E.Rivera, M.Morari, S.Skogetstad. 1986. Internal model control for PID controller design. *Industrial and Engineering Chemistry, Process Design and Development*. 25252-265.
- [16] A.Emadi. 2005. *Energy-Efficient Electric Motor*. Marcel Dekker, New York